Karadeniz Fen Bilimleri Dergisi, 13(4), 1581-1594, 2023. DOI: 10.31466/kfbd.1323317

KFBD

Karadeniz Fen Bilimleri Dergisi
The Black Sea Journal of Sciences
ISSN (Online): 2564-7377 https://dergipark.org.tr/tr/pub/kfbd

Araştırma Makalesi / Research Article

Exploring Microstructure and Bending Strength of Al_2O_3 Ceramics Doped with Sm_2O_3 Rare-Earth Oxide: Impact of Volume Ratios and Sintering Temperatures

Seda TAŞDEMİR[1], Betül KAFKASLIOĞLU YILDIZ[2*], Elif IŞIK[3], Yahya Kemal TÜR[4]

Abstract

The effects of low amounts (0, 0.1, 0.3, 0.5, 0.8, 1, 2vol%) of Sm_2O_3 on the densification, microstructure, and bending strength of Al_2O_3 were studied for different sintering temperatures. Sm_2O_3 and Al_2O_3 powders were mixed by ball milling, and Al_2O_3-Sm_2O_3 ceramics were prepared by dry and cold isostatic pressing in disc form before pressureless sintering at 1550°C and 1600°C/2 h in the air, separately. Sm_2O_3 reacted with Al_2O_3 by forming $SmAlO_3$. The rod-like morphology of the $SmAlO_3$ was generally achieved for 0.8 and 1vol% Sm_2O_3 for sintering at 1600°C, whereas the rod-like form was more obvious for the samples sintered at 1550°C. Similar relative densities were attained for all Sm_2O_3 ratios at both sintering temperatures, but the Al_2O_3 sintered at 1550°C exhibited higher densification than the Al_2O_3 sintered at 1600°C. The strength values were close, while a strength increase of about 5% was obtained for 0.5 vol% Sm_2O_3 containing ceramics sintered at 1600°C caused by the higher densification compared to the Al_2O_3. The strength showed a prominent drop above the ratio of 0.1 vol% Sm_2O_3 for sintering at 1550°C. The addition of present amounts of Sm_2O_3 did not have a significant effect on the mechanical properties of Al_2O_3 but it changed the microstructure.

Keywords: Al_2O_3, Sm_2O_3, microstructure, mechanical properties.

Sm_2O_3 Nadir Toprak Oksit Katkılı Al_2O_3 Seramiklerinin Mikro Yapısının ve Eğilme Dayanımının İncelenmesi: Hacim Oranlarının ve Sinterleme Sıcaklıklarının Etkisi

Öz

Düşük miktarlarda (0, 0,1, 0,3, 0,5, 0,8, 1, 2 hac.%) Sm_2O_3'ün Al_2O_3'ün yoğunlaşma, mikroyapı ve eğilme dayanımı üzerindeki etkileri farklı sinterleme sıcaklıkları için incelenmiştir. Sm_2O_3 ve Al_2O_3 tozları bilyeli öğütme ile karıştırılmış ve Al_2O_3-Sm_2O_3 seramikleri, ayrı ayrı 1550°C'de ve 1600°C/2 saat havada basınçsız sinterlemeden önce disk formunda kuru ve soğuk izostatik presleme ile hazırlanmıştır. Sm_2O_3, Al_2O_3 ile reaksiyona girerek $SmAlO_3$ oluşturmuştur. $SmAlO_3$'ün çubuk benzeri morfolojisi, 1600°C'de sinterleme için genel olarak hacimce %0,8 ve 1 Sm_2O_3 için elde edilirken, 1550°C'de sinterlenen numunelerde çubuk benzeri form daha belirgin olmuştur. Her iki sinterleme sıcaklığında da tüm Sm_2O_3 oranları için benzer relatif yoğunluklar elde edilmiştir ancak 1550°C'de sinterlenen Al_2O_3, 1600°C'de sinterlenen Al_2O_3'e göre daha yüksek yoğunlaşma sergilemiştir. 1600°C'de sinterlenen hac.%0,5 Sm_2O_3 içeren seramiklerde, Al_2O_3'e göre daha yüksek yoğunlaşma sebebiyle yaklaşık %5'lik bir mukavemet artışı elde edilirken, mukavemet değerleri genelde birbirine yakın olmuştur. Mukavemet, 1550°C'de sinterleme için hac.%0,1 Sm_2O_3 oranının üzerinde belirgin bir düşüş göstermiştir. Mevcut miktarlarda Sm_2O_3 ilavesinin Al_2O_3'ün mekanik özellikleri üzerinde önemli bir etkisi olmamıştır, ancak mikroyapıyı değiştirmiştir.

Anahtar Kelimeler: Al_2O_3, Sm_2O_3, mikroyapı, mekanik özellikler.

[1]Sivas University of Science and Technology, Institute of Graduate Studies, Defense Technology Programme, Sivas, Turkey, sbzkrt7016@gmail.com
[2,3]Sivas University of Science and Technology, Metallurgical and Materials Engineering Department, Sivas, Turkey, bkyildiz@sivas.edu.tr elif.isik@sivas.edu.tr
[4]Gebze Technical University, Materials Science and Engineering Department, Kocaeli, Turkey, yktur@gtu.edu.tr

[1]https://orcid.org/0000-0002-8910-1486 [2]https://orcid.org/0000-0002-6527-2918 [3]https://orcid.org/0000-0001-8289-9512
[4]https://orcid.org/0000-0002-9521-8875

***Sorumlu Yazar/Corresponding Author**

Geliş/Received: 05.07.2023 **Kabul/Accepted:** 21.09.2023

1. Introduction

Al_2O_3 ceramics can be counted as a classic representative of advanced ceramics. The physical properties of these ceramics are mostly desirable for structural applications such as in defense industries, aerospace, and biomedical, mainly while the environmental conditions are specifically severe (Shuai et al., 2020; Dresch et al., 2021; Ma et al., 2019). Nevertheless, the fracture toughness and flexural strength of Al_2O_3 ceramics are low among the most commonly used technical ceramics like Si_3N_4 and SiC (Hazell, 2016; Dresch et al., 2021; Flinders et al., 2005). This can be seen as a disadvantage when it comes to the use of these materials in critical applications (Huang and Chen, 2016; Kafkaslıoğlu Yıldız and Tür, 2021). The additives are greatly significant for the achievement of the sintering and, hence, for the enhancement of the mechanical properties (Lartigue-Korinek et al., 2002; Shi et al., 2020; Harun et al., 2012; Aktas et al., 2016). Latterly, various rare earth element oxides have been commonly used as sintering additives for Al_2O_3 ceramics to enhance the densification process and improve mechanical properties (Rani et al., 2004). By using rare earth oxides, it is probable to decrease the sintering temperature of ceramics and enhance their microstructures. Rare earth oxides including Sm_2O_3, La_2O_3, Dy_2O_3, Y_2O_3, CeO_2, Er_2O_3, and Eu_2O_3 are commonly employed (Shi et al., 2020; Yijun et al., 2010; Ge et al., 2019; Aktas, Tekeli, Kucuktuvek, 2014; Aktas, Tekeli, Salman, 2014). Samarium (III) oxide (Sm_2O_3) is a light rare earth element oxide with a melting temperature of over 2000°C, making it a suitable additive for the production of ceramics with enhanced sintering properties (Shi et al., 2020). Sm_2O_3 rare earth oxides react with Al_2O_3 by forming the $SmAlO_3$ phase at high sintering temperatures, consistent with their phase diagram (Mizuno et al., 1977). In Al_2O_3-Sm_2O_3 ceramic systems, the formed $SmAlO_3$ phase elongates along the growth direction, and corresponding Al_2O_3-$SmAlO_3$ ceramic composites have high mechanical properties (toughness, flexural strength) since this phase formed can act as short fiber reinforcement (Shi et al., 2020).

Shi et al. studied 20 vol.% Ti and (0-2.0 at%) $SmAlO_3$ containing Al_2O_3 ceramics in their study and obtained high toughness and bending strength values as a result of strengthening and toughening effects with the support of $SmAlO_3$ phase (Shi et al., 2020). Also, Yijun et al. studied the effect of different rare earth oxides (Y_2O_3, La_2O_3, and Sm_2O_3) on the mechanical properties of Al_2O_3 ceramics. The addition of rare-earth oxides enhanced the mechanical properties of Al_2O_3 especially for 0.5 wt% Sm_2O_3 content by way of grain size refinement and grain boundary strengthening mechanisms (Yijun et al., 2010). There are only a few studies in the literature examining the mechanical properties of Sm_2O_3 doped Al_2O_3 ceramics and the studies are mainly related to the creep and mechanical behavior of the eutectic composition (26 % Sm_2O_3+ 74% Al_2O_3) (Londaitzbehere et al., 2017; Ma et al., 2019). Therefore, in this work, the effects of different low amounts (0.1, 0.3, 0.5, 0.8, 1, 2vol%) of Sm_2O_3

rare-earth oxide additive on the densification, microstructure, and bending strength of Al_2O_3 ceramics were investigated to reveal the efficiency of the $SmAlO_3$ secondary phase on these properties. The morphology of the formed phase and the mechanical properties (elastic modulus and strength) were investigated depending on the additive ratio and the sintering temperature.

2. Materials and Methods

To produce Al_2O_3-Sm_2O_3 ceramics, a high purity α-Al_2O_3 powder (Alfa Aesar, 99.95% purity, 0.25-0.45 μm), Sm_2O_3 powder (99.95%, 50 nm, Nanografi, Turkey), polyacrylic acid (MSE Tech Co. Ltd., Turkey) as a dispersant, polyvinyl alcohol (Sigma Aldrich) as polymer binder, and glycerol as plasticizer (Sigma Aldrich) were used as starting powders and chemicals. High-purity powders were used to examine the effect of the Sm_2O_3 additive on densification. Different amounts of Sm_2O_3 powder (equivalent to 0, 0.1, 0.3, 0.5, 0.8, 1, 2 vol%) and Al_2O_3 powder were mixed in an HDPE bottle with distilled water and dispersant (0.5wt%) by ball milling, separately. After 1.5wt% binder + 0.5wt% plasticizer aqueous solution addition to the ball milled powder mixture, the slurry was dried on a hot plate and in a drying oven at 70°C. The dried powder mixture was crushed and sieved through a 170 mesh screen. Then, the powder mixtures were pressed under a uniaxial applied pressure of 40 MPa in a 35 mm diameter cylinder mold. Subsequently, the green bodies taken into the vacuum in a latex material were exposed to cold isostatic pressing under 200 MPa pressure. The prepared specimens were pressureless sintered at 1550°C and 1600°C in air separately with a heating rate of 5°/min, while the binder burn-out process was carried out at 600°C with a heating rate of 2°/min in an air atmosphere. The specimens were also grinded using a single-sided lapping machine with SiC abrasive powder to make equal thicknesses of the pellets with ±0.05 mm tolerance for compatibility with the mechanical tests.

The phases present in the sintered specimens were characterized by the X-ray diffraction method (Bruker® D8 Advance) for 2θ between 10° and 90°. The bulk densities were measured by direct measurement of weight and macroscopic dimensions precisely with a micrometer and a caliper. The theoretical densities of the ceramics were determined by the rule of mixtures (Hossen et al., 2014). After grinding and polishing, the specimens were thermally etched at 100°C below the sintering temperatures for 90 min for microstructural exploration. The grain morphology and average Al_2O_3 grain size were characterized by using scanning electron microscopy (TESCAN Mira3 XMU, Czechia) equipped with energy-dispersive X-ray spectroscopy (EDS) to investigate the chemistry of the phases. The grain size measurements were performed with the linear intercept method where more than 100 intercepts were counted for each Al_2O_3-Sm_2O_3 ceramic with different Sm_2O_3 content.

The elastic modulus of the polished specimens was measured via an impulse excitation technique (GrindoSonic® Mk5) appropriate for ASTM E 1876 standard to disc-formed samples. The bending strength test of the Al_2O_3-Sm_2O_3 ceramics was carried out using the equibiaxial flexural strength test procedure consistent with ASTM C 1499 at a loading rate of 0.3 mm/min with 23.9 mm support ring and 9.8 mm load ring test configuration for fifteen specimens at ambient temperature using a universal test machine (Instron-5569, USA).

3. Findings and Discussion

XRD diffraction patterns of the Al_2O_3-Sm_2O_3 ceramics prepared with different Sm_2O_3 volume ratios are given in Figure 1. A single graph is given as the XRD diffraction patterns are almost the same for the samples sintered at 1550°C and 1600°C. In the graph, "A" indicates Al_2O_3 peaks while "SA" refers to $SmAlO_3$ peaks. The presence of Al_2O_3 (α-type, hexagonal corundum) and $SmAlO_3$ phase (orthorhombic) formed with the reaction of Al_2O_3 and Sm_2O_3 were detected. No other extra phase was observed, and $SmAlO_3$ peaks became evident, especially after 0.5vol% Sm_2O_3 ratio. When the amount of Sm_2O_3 increased, the peaks of the $SmAlO_3$ phase gradually became apparent.

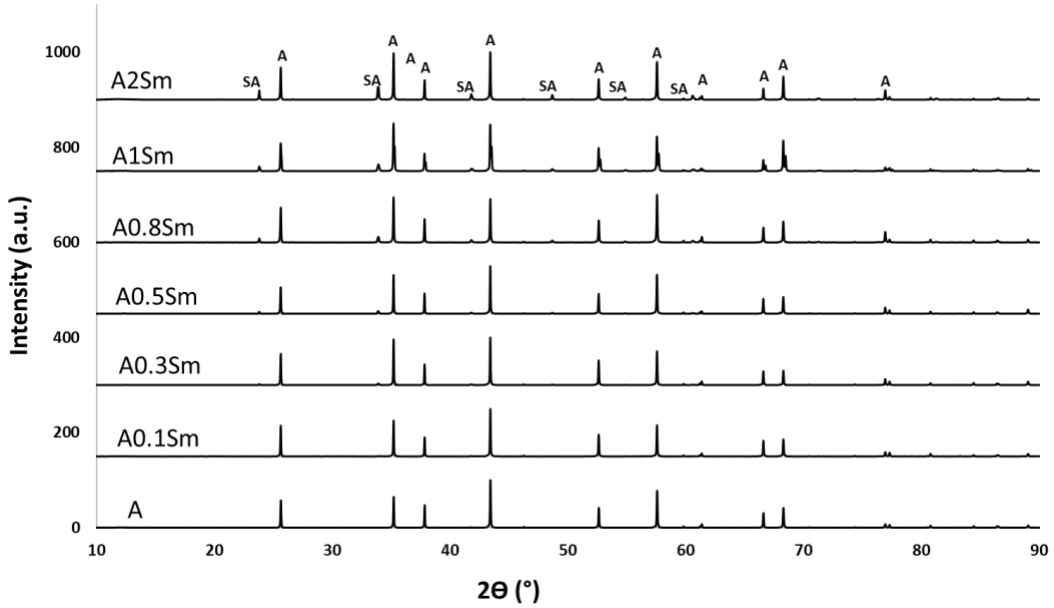

Figure 1. The XRD diffraction patterns of the Al_2O_3-Sm_2O_3 ceramics prepared with different Sm_2O_3 volume ratios.

The relative density, Al_2O_3 grain size values, and mechanical properties are shown depending on the Sm_2O_3 amount and the sintering temperature in Table 1. The theoretical density values were estimated by the rule of mixtures, and the relative densities were calculated from the ratio of the bulk densities to the theoretical densities. Almost similar relative density values were obtained in the

Al_2O_3-Sm_2O_3 ceramics for all the Sm_2O_3 ratios at both sintering temperatures. However, the pure Al_2O_3 samples sintered at 1550°C exhibited higher densification than the samples sintered at 1600°C. In general, it was observed that the addition of Sm_2O_3 for sintering at 1550°C did not affect the densification of Al_2O_3 considerably. For 1600°C, it can be thought that there is a slight increase in the relative density values after the addition of the Sm_2O_3 additive. Shi et al. stated in their study that after Sm_2O_3 is added, it dissolves into Al_2O_3 by taking up the site originally occupied by Al^{3+} cations with Sm^{3+} cations, increasing the concentration of aluminum vacancies. A higher concentration of aluminum vacancies encourages mass transformation and pores to be eliminated, resulting in significant densification (Shi et al., 2020). This was not determined for this study. It would be useful to view the SEM images of the thermally etched samples in both Figure 2 and Figure 3 to understand the discrepancy. In these figures, "A" denotes the pure alumina, and "Sm" states the samples containing Sm_2O_3, while the number in front of the letter Sm denotes the amount of Sm_2O_3 added. Dark gray areas belong to Al_2O_3 grains in the SEM figures.

The Al_2O_3 powder used in this study is a very high-purity powder and does not contain any grain growth inhibitors and sintering aids such as MgO. In various studies using rare earth oxides such as Sm_2O_3, it has been found that the densification effect of these rare earth additives is more effective in the presence of sintering aids up to the sintering temperatures (Rani et al., 2004). When the sintering temperature rises from 1550°C to 1600°C, inhomogeneous particle sizes can be seen for the pure Al_2O_3 in Figure 3 with both fine grains and too large grains. Abnormal grain growth was seen in the pure Al_2O_3 samples sintered at 1600°C. In addition to abnormal grain growth, the presence of large porosities in these samples was also detected in the SEM images. Based on these results, it was decided that 1600°C is not a suitable sintering temperature for the powder used and the present production conditions. For sintering at 1550°C, the pure Al_2O_3 grains were more homogeneous, and an average grain size of 1.8 μm was obtained as given in Table 1. With the addition of Sm_2O_3, the grains grew more homogeneously but reached quite large sizes about 25-30 μm at both sintering temperatures. No correlation could be specified between the sintering temperature, the Sm_2O_3 ratios and the grain size. It is thought that this disorder is related to the formation of the secondary $SmAlO_3$ phase and its distribution differs from region to region in the specimens.

The presence of the $SmAlO_3$ phase in rod-like form can be easily seen in white color in SEM images for 0.3, 0.5, 0.8, and 1vol%Sm_2O_3 content in Figure 2. However, it is seen that this rod-like form becomes spherical in samples containing 2vol% Sm_2O_3 for both sintering temperatures. In the samples sintered at 1600°C, the rod-like form was obtained mostly for 0.8 and 1vol% Sm_2O_3 ratios. On the contrary, the rod-like form was more pronounced for the samples sintered at 1550°C. These results showed that the morphology of the $SmAlO_3$ phase was related to the Sm_2O_3 amount and the sintering temperature.

Table 1: Densification, matrix grain size, and mechanical properties of the prepared Al_2O_3-Sm_2O_3 ceramics for different sintering temperatures.

Sm_2O_3 content (vol%)	Sintering Temperature (°C)	Relative Density (%)	Elastic Modulus (GPa)	Bending Strength (MPa)	Average Al_2O_3 grain size (mm)
0	***1550***	***98.4 ± 0.3***	***390 ± 3***	***279 ± 27***	***1.8***
0.1	1550	98.5 ±0.2	388 ± 2	205 ± 15	29.5
0.3	1550	98.4 ± 0.4	389 ± 3	198 ± 19	25.7
0.5	1550	98.6 ± 0.3	389 ± 5	193 ± 17	30.2
0.8	1550	98.6 ± 0.3	390 ± 2	189 ± 14	36.5
1	1550	98.4 ± 0.4	385 ± 6	191 ± 12	26.9
2	1550	98.2 ± 0.2	383 ± 7	177 ± 13	27.4
0	***1600***	***97.8 ± 0.5***	***381 ± 5***	***188 ± 15***	***8.3***
0.1	1600	98.1 ± 0.5	386 ± 5	195 ± 12	21.1
0.3	1600	98.3 ± 0.4	385 ± 5	192 ± 8	26.6
0.5	1600	98.3 ± 0.4	386 ± 3	197 ± 14	30.2
0.8	1600	98.4 ± 0.3	388 ± 3	190 ± 11	29.4
1	1600	98.2 ± 0.3	384 ± 3	185 ± 13	33.4
2	1600	98.2 ± 0.4	383 ± 5	175 ± 15	32.5

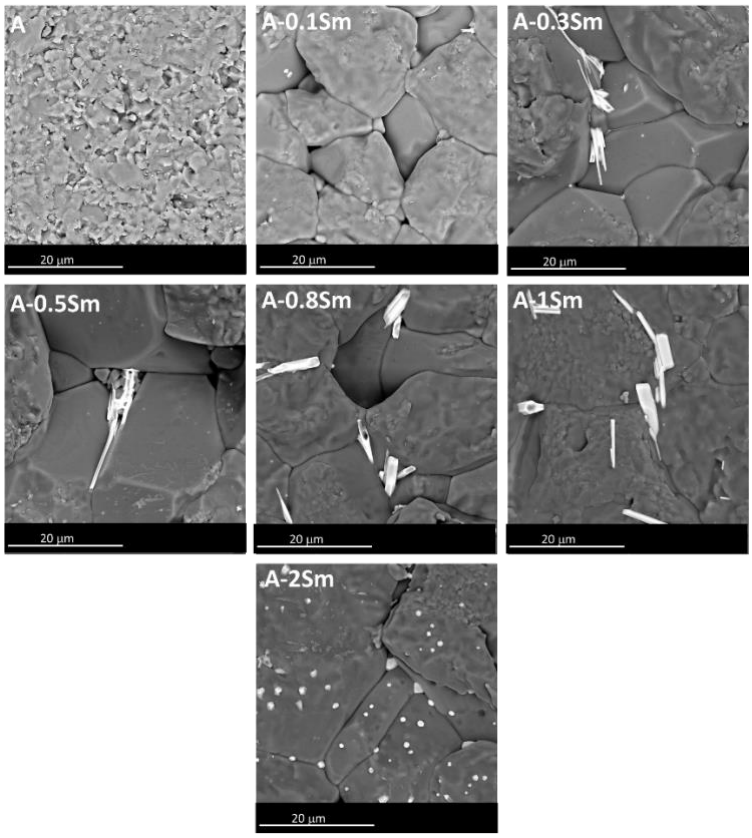

Figure 2. SEM images of the thermally etched Al_2O_3-Sm_2O_3 ceramics sintered at 1550°C.

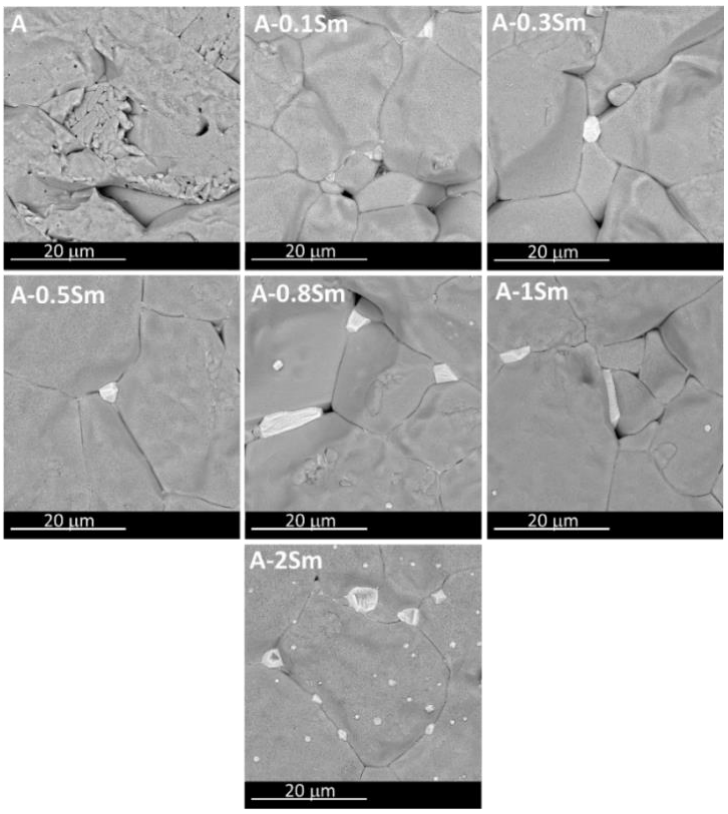

Figure 3. SEM images of the thermally etched Al_2O_3-Sm_2O_3 ceramics sintered at 1600°C.

The SEM-EDX mapping results of the thermally etched Al_2O_3-1vol%Sm_2O_3 containing ceramic are presented in Figure 4. The turquoise areas belong to O elements, while the yellow and purple regions indicate Al and Sm elements, respectively. From the SEM-EDX results, it was more clearly determined that the phase in rod-like form belongs to $SmAlO_3$ particles that were mostly positioned at the triple junctions and grain boundaries.

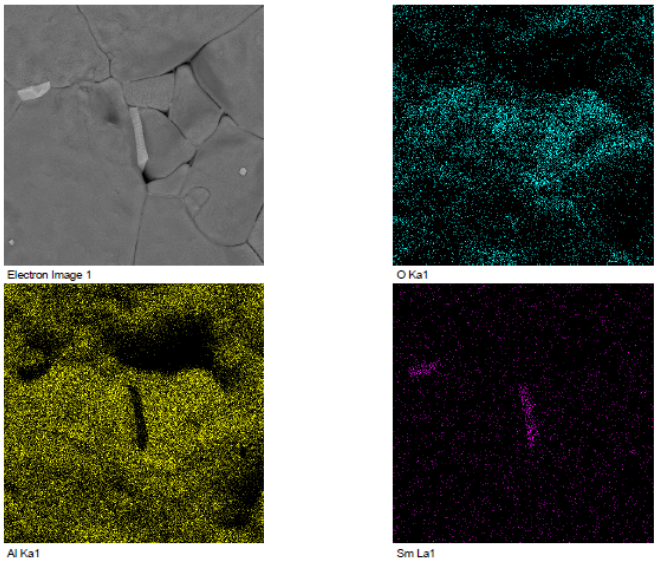

Figure 4. SEM-EDX mapping images of the thermally etched Al_2O_3- 1vol%Sm_2O_3 containing ceramic.

When the produced ceramics are examined in terms of mechanical properties, it is seen that the elastic modulus results were nearly the same for all the produced ceramics. Since the relative density results were similar, it can be thought that the elastic modulus values were also similar as the densification ratio affects the elastic modulus of a ceramic material. It is stated in the literature that the elastic modulus of a material is greatly affected by porosity (Feng et al., 2019). Therefore, the lowest elastic modulus was obtained for the pure Al_2O_3 sintered at 1600°C with a value of 381 GPa.

The bending strength values of Al_2O_3-Sm_2O_3 ceramics as a function of Sm_2O_3 volume content are given in Figure 5 and Table 1 for both sintering temperatures. Although the strength values are generally close to each other, a strength increase of about 5% was obtained for 0.5 vol% Sm_2O_3 containing ceramics sintered at 1600°C due to the higher densification compared to the pure Al_2O_3 sintered at 1600°C. For the 2vol% Sm_2O_3 ratio, a decrease of ~7% was observed in the strength for 1600°C. Although the strength showed further decline above the ratio of 0.1 vol% Sm_2O_3, the strength values were nearly similar up to 2vol% Sm_2O_3 content for the other ratios (0.3, 0.5, 0.8, 1vol%) for sintering at 1550°C. It is thought that the more significant decrease in strength for the 2vol% Sm_2O_3 ratio at both sintering temperatures is related to the morphology of the $SmAlO_3$ phase becoming completely spherical from the rod-like form at this ratio by including the $SmAlO_3$ phase embedded in the Al_2O_3 grains. Besides, the reason for the decrease in bending strength with the addition of Sm_2O_3 is the presence of quite large Al_2O_3 grains for sintering at 1550°C. It is stated that the bending strength of a ceramic material relates strongly to its grain size and flaw size. Larger grains introduce greater flaws, which results in lower strength. (Tuan et al., 2008). Therefore, larger Al_2O_3 grain sizes resulted in lower strength values compared to the pure Al_2O_3 for Sm_2O_3 containing samples with similar densification for sintering at 1550°C. Since the pure Al_2O_3 sintered at 1600°C has abnormally grown grains, there was no significant difference in strength between the samples containing Sm_2O_3 sintered at this temperature. On the other hand, a direct relationship between the grain size and the bending strength change could not be determined for all the samples containing the Sm_2O_3 additive since the grain size values varied. For example, for the samples sintered at 1600°C, 197 MPa strength was measured in the sample containing 0.5vol% Sm_2O_3 with a grain size of approximately 30 μm, while almost the same 195 MPa strength was obtained in the sample containing 0.1vol% Sm_2O_3 with a grain size of 21 μm.

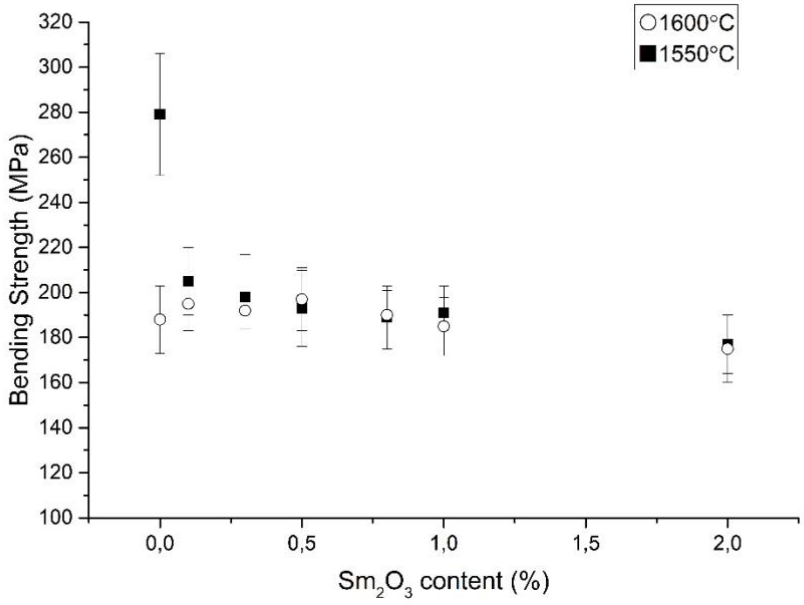

Figure 5. The bending strength of Al_2O_3-Sm_2O_3 ceramics as a function of Sm_2O_3 volume content for the sintering temperature.

In order to interpret the fracture strength behavior depending on the microstructure, it is also necessary to examine the fracture surface SEM images. Figure 6 shows the fracture surface of the pure Al_2O_3 sintered at 1550°C. Although the fracture mode was mostly intergranular for the small grains, it is seen that the coarser grains were fractured by cleavage. It is stated that when the grain size of a ceramic material is enhanced, the fracture mode alters from intergranular to cleavage (transgranular). As ceramics often have fine grain sizes, their grain boundaries have a larger surface area and more energy than the grains themselves, which causes intergranular fracture most of the time. However, with an increase in grain size, grain boundary area decreases thus changing the fracture mode to cleavage (Kambale et al., 2019).

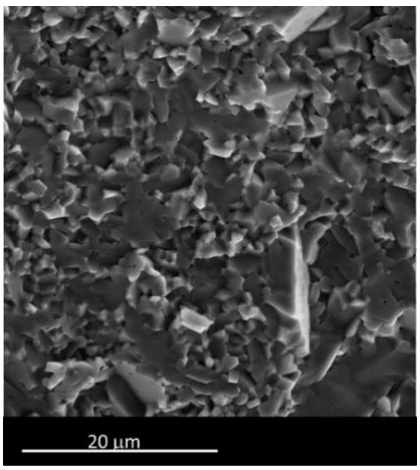

Figure 6. SEM image of the fracture surface of the Al_2O_3 sintered at 1550°C.

SEM images of the fracture surfaces of the Al_2O_3-Sm_2O_3 ceramics for both sintering temperatures are also given in Figure 7 and Figure 8, separately. For sintering at 1550°C, the Al_2O_3-Sm_2O_3 ceramics for all the Sm_2O_3 additive ratios showed almost completely transgranular fracture mode differently from the pure Al_2O_3 sintered at the same temperature. This can clearly be attributed to the much larger size of the Al_2O_3 grains in the Al_2O_3-Sm_2O_3 ceramics compared to the pure Al_2O_3. The possible effect of the formed $SmAlO_3$ phase on the fracture behavior could not be identified due to the effect of large grains. A similar fracture behavior as transgranular was also valid for the Al_2O_3-Sm_2O_3 ceramics sintered at 1600°C. In addition, the difference in the fracture mode for the pure Al_2O_3 with abnormal growth grains for sintering at 1600°C is seen compared to Figure 6 for sintering at 1550°C.

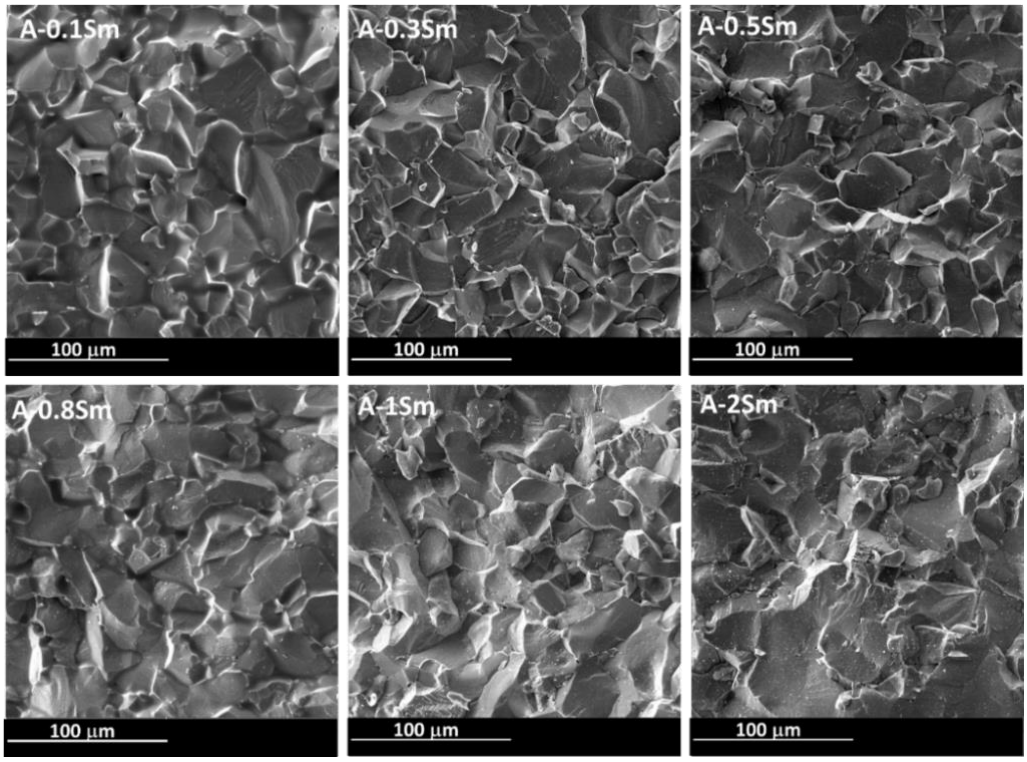

Figure 7. SEM images of the fracture surfaces of the Al_2O_3-Sm_2O_3 ceramics sintered at 1550°C.

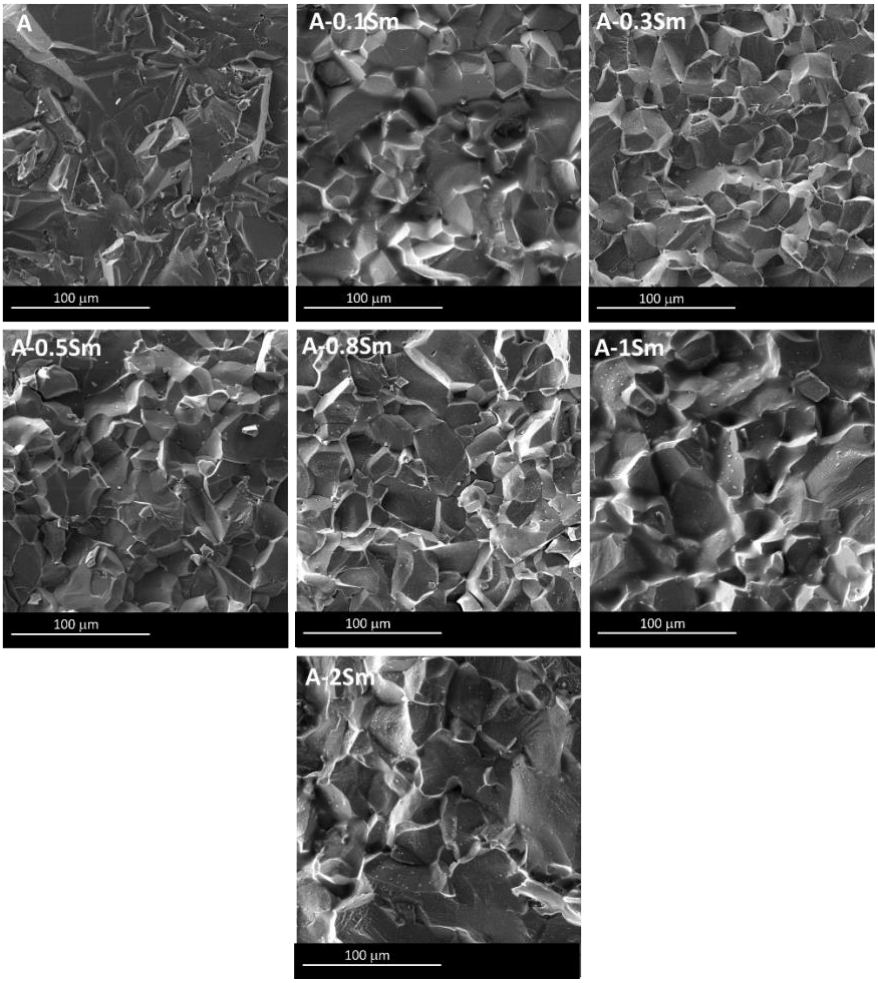

Figure 8. SEM images of the fracture surfaces of the Al_2O_3-Sm_2O_3 ceramics sintered at 1600°C.

4. Conclusions

In the present investigation, the effects of different amounts (0, 0.1, 0.3, 0.5, 0.8, 1, 2vol%) of Sm_2O_3 additive on the densification, microstructure, and mechanical properties (elastic modulus and bending strength) of Al_2O_3 ceramics were studied for different sintering temperatures. The fabrication procedure involved ball milling of nano-sized Sm_2O_3 powder with the Al_2O_3 powder in proper volume ratios and followed by pressureless sintering at 1550°C and 1600°C for two hours in the air separately after uniaxially dry and cold isostatic pressing. Sm_2O_3 reacted with the Al_2O_3 by forming the $SmAlO_3$ phase at the sintering temperatures and the existence of the $SmAlO_3$ phase was confirmed by the XRD analysis. In the samples sintered at 1600°C, the rod-like form of the $SmAlO_3$ phase was obtained mostly for 0.8 and 1vol% Sm_2O_3 ratios while the rod-like form of the phase was more evident for the samples sintered at 1550°C. Similar densification behavior was obtained in the Al_2O_3-Sm_2O_3 ceramics for all Sm_2O_3 ratios at both sintering temperatures. Nevertheless, the pure Al_2O_3 sintered at 1550°C exhibited higher densification than the samples sintered at 1600°C. Since the relative density results were similar, the elastic modulus values were also parallel. Though the

bending strength values were in general close to each other, a strength increase of about 5% was obtained for 0.5 vol% Sm_2O_3 containing ceramics sintered at 1600°C caused by the higher densification compared to the pure Al_2O_3. The strength values showed a further drop above the ratio of 0.1 vol% Sm_2O_3, but they were nearly similar up to 2vol% Sm_2O_3 content for the other ratios (0.3, 0.5, 0.8, 1vol%) for sintering at 1550°C. For both sintering temperatures, the Al_2O_3-Sm_2O_3 ceramics in all Sm_2O_3 additive ratios showed transgranular fracture mode. Based on the results obtained, it was observed that the addition of Sm_2O_3 to the relevant ratios did not cause a remarkable increase in the mechanical properties of the Al_2O_3 ceramic but changed the microstructure.

Acknowledgements

This work was supported by the Scientific and Technical Research Council of Turkey-TUBITAK through the project no 122M179. This article was also prepared from the studies of Seda Taşdemir for her master's degree at Sivas University of Science and Technology, Defense Technology Programme. The authors thank Dr. Halil İbrahim Çetintaş and Adem Şen for their assistance in the SEM and XRD analysis of this study, respectively.

Authors' Contributions

ST: Experimental, Investigation, Visualization. BKY: Conceptualization, Investigation, Experimental, Writing - review and editing. EI: Experimental, Investigation. YKT: Conceptualization, Writing - review and editing.

Statement of Conflicts of Interest

There is no conflict of interest between the authors.

Statement of Research and Publication Ethics

The author declares that this study complies with Research and Publication Ethics.

References

Aktas, B., Tekeli, S., and Kucuktuvek, M. (2014). Grain growth and sinterability in Er_2O_3-doped cubic zirconia (c-ZrO_2). *International Journal of Materials Research,* 105,2,208-214. https://doi.org/10.3139/146.110999.

Aktas, B., Tekeli, S., and Salman, S. (2014). Synthesis and Properties of La_2O_3-Doped 8 mol% Yttria-Stabilized Cubic Zirconia. *Journal of Materials Engineering and Performance*, 23,294–301. https://doi.org/10.1007/s11665-013-0736-3.

Aktas, B., Tekeli, S., and Salman, S. (2016). Improvements in microstructural and mechanical properties of ZrO_2 ceramics after addition of BaO. *Ceramics International*, 42, 3849–3854. http://dx.doi.org/10.1016/j.ceramint.2015.11.049.

Dresch, A. B., Venturini, J., and Bergmann, C. P. (2021). Improving the flexural-strength-to-density ratio in alumina ceramics with the addition of silicon nitride. *Ceramics International*, 47,3964–3971. https://doi.org/10.1016/j.ceramint.2020.09.260

Feng, L., Fahrenholtz, W. G., Hilmas, G. E., Watts, J., and Zhou, Y. (2019). Densification, microstructure, and mechanical properties of ZrC–SiC ceramics. *Journal of the American Ceramic Society*, 102, 5786–5795. https://doi.org/10.1111/jace.16505

Flinders, M., Ray, D., Anderson, A., and Cutler, R. A. (2005). High-toughness silicon carbide as armor. *Journal of the American Ceramic Society*, 88, 2217–2226. https://doi.org/10.1111/j.1551-2916.2005.00415.x

Ge, X. Z, Ge, Q., Ge, X. S., Ji, D. H., Huang, Y., Zhang, Z. L., and Zhang, H. B. (2019). Influence of La_2O_3 Addition on Microstructure and Mechanical Properties of Al_2O_3 Ceramics. *Materials Science Forum Volume*, 956, 69-77. https://doi.org/10.4028/www.scientific.net/MSF.956.69

Harun, Z., Ismail, N., and Badarulzaman, N. (2012). Effect of MgO additive on microstructure of Al_2O_3, *Advanced Materials Research*, 335-339.https://doi.org/10.4028/www.scientific.net/AMR.488-489.335

Hazell, P. J., (2016). *Armour: materials, Theory, and Design* (1st ed.). Boca Raton: CRC Press.

Huang, C. Y., and Chen, Y. L. (2016). Effect of mechanical properties on the ballistic resistance capability of Al_2O_3-ZrO_2 functionally graded materials. *Ceramics International*, 42,12946–12955. https://doi.org/10.1016/j.ceramint.2016.05.067

Kafkaslıoğlu Yıldız, B., and Tür, Y. K. (2021). Effect of ZrO_2 content on the microstructure and flexural strength of Al_2O_3–ZrO_2 composites with the stored failure energy-fragmentation relations. *Ceramics International*, 47, 34199–34206. https://doi.org/10.1016/j.ceramint.2021.08.329

Kambale, K. R. Mahajan, A., and Butee, S. P. (2019). Effect of grain size on the properties of ceramics, *Metal Powder Report,* Volume 74, 3. https://doi.org/10.1016/j.mprp.2019.04.060

Lartigue-Korinek, S., Carry, C., and Priester, L. (2002). Multiscale aspects of the influence of yttrium on microstructure, sintering and creep of alumina. *Journal of the European Ceramic Society,* 22, 1525-1541. https://doi.org/10.1016/S0955-2219(01)00471-X

Londaitzbehere, L., Lartigue-Korinek, S., and Mazerolles, L. (2017). Microstructure, interfaces and creep behavior of Al_2O_3-Sm_2O_3(ZrO_2) eutectic ceramic composites. *Journal of Materials Science*, 52, 5489-5502. https://doi.org/10.1007/s10853-016-0726-6

Ma, Y. H., Ouyang, J. H., Wang, Z. G., Hennich, A., Wang, Y. H., Wang, Y. J., and Liu, Z. G. (2019). Insights into intragranular precipitation and strengthening effect in Al_2O_3/$SmAlO_3$ ceramic with eutectic composition. *Materials Science & Engineering A,* 754, 382–389. https://doi.org/10.1016/j.msea.2019.03.091

Mizuno, M., Yamada, T., and Noguchi, T. (1977). Phase diagram of the system Al_2O_3-Sm_2O_3 at high Temperatures. *Journal of the Ceramic Association Japan*, 85, 374-379.

Moazzam Hossen, M., Chowdhury, F. U. Z., Gafur, M. A., Abdul Hakim, A. K. M., and Nasrin, S. (2014). Investigation of mechanical properties of Al_2O_3-20wt%ZrO_2 composites as a function of sintering temperature. *European Scientific Journal,* 10(9), 399-411. https://doi.org/10.19044/esj.2014.v10n9p%25p

Rani, D. A., Yoshizawa, Y., Hirao, K., and Yamauchi, Y. (2004). Effect of Rare-Earth Dopants on Mechanical Properties of Alumina. *Journal of the American Ceramic Society,* 87(2)289–92. https://doi.org/10.1111/j.1551-2916.2004.00289.x

Shi, S., Cho, S., Goto, T., and Sekino, T. (2020). Ti and $SmAlO_3$ co-affected Al_2O_3 ceramics: Microstructure, electrical and mechanical properties. *Journal of Alloys and Compounds*, 835, 155427. https://doi.org/10.1016/j.jallcom.2020.155427

Shuai, X., Zeng, Y., Li, P., and Chen, J. (2020). Fabrication of fine and complex lattice structure Al_2O_3 ceramic by digital light processing 3D printing technology. *Journal of Materials Science*, 55, 6771–6782. https://doi.org/10.1007/s10853-020-04503-y

Tuan, W. H., Chen, J. R., and Ho, C. J. (2008). Critical zirconia amount to enhance the strength of alumina, *Ceramics International*, 34, 2129–2135. https://doi.org/10.1016/j.ceramint.2007.08.013

Yijun, Y., Chuncheng, L., Ling, W., Xiaolong, J., and Tai, Q. (2010). Mechanical behaviors of alumina ceramics doped with rare-earth oxides. *Rare Metals*, 29, 456. https://doi.org/10.1007/s12598-010-0149-5